

# The Geomagnetic Field at the Paleozoic/Mesozoic and Mesozoic/Cenozoic Boundaries and Lower Mantle Plumes

D. M. Pechersky

*Schmidt Institute of Physics of the Earth, Russian Academy of Sciences, Bol'shaya Gruzinskaya ul. 10, Moscow, 123995 Russia*

Received February 6, 2006

**Abstract**—The data on the amplitude of variations in the direction and paleointensity of the geomagnetic field and the frequency of reversals throughout the last 50 Myr near the Paleozoic/Mesozoic and Mesozoic/Cenozoic boundaries, characterized by peaks of magmatic activity of Siberian and Deccan traps, and data on the amplitude of variations in the geomagnetic field direction relative to contemporary world magnetic anomalies are generalized. The boundaries of geological eras are not fixed in recorded paleointensity, polarity, reversal frequency, and variations in the geomagnetic field direction. Against the background of the “normal” field, nearly the same tendency of an increase in the amplitude of field direction variations is observed toward epicenters of contemporary lower mantle plumes; Greenland, Deccan, and Siberian superplumes; and world magnetic anomalies. This suggests a common origin of lower mantle plumes of various formation times, world magnetic anomalies, and the rise in the amplitude of geomagnetic field variations; i.e., all these phenomena are due to a local excitation in the upper part of the liquid core. Large plumes arise in intervals of the most significant changes in the paleointensity (drops or rises), while no correlation exists between the plume generation and the reversal frequency: times of plume formation correlate with the very diverse patterns of the frequency of reversals, from their total absence to maximum frequencies, implying that world magnetic anomalies, variations in the magnetic field direction and paleointensity, and plumes, on the one hand, and field reversals, on the other, have different sources. The time interval between magmatic activity of a plume at the Earth’s surface and its origination at the core–mantle boundary (the time of the plume rise toward the surface) amounts to 20–50 Myr in all cases considered. Different rise times are apparently associated with different paths of the plume rise, “delays” in the plume upward movement, and so on. The spread in “delay” times of each plume can be attributed to uncertainties in age determinations of paleomagnetic study objects and/or the natural remanent magnetization, but it is more probable that this is a result of the formation of a series of plumes (superplumes) in approximately the same region at the core–mantle boundary in the aforementioned time interval. Such an interpretation is supported by the existence of compact clusters of higher field direction amplitudes between 300 and 200 Ma that are possible regions of formation of world magnetic anomalies and plumes.

PACS numbers: 91.25.Dx

DOI: 10.1134/S1069351307100072

## INTRODUCTION

If lower mantle plume magmatism originates at the core–mantle boundary, it must be reflected in the behavior of the geomagnetic field, generated by processes in the liquid core of the Earth. Researchers have repeatedly written that the plume formation and the geomagnetic field behavior are interrelated, noting, for example, that the maximum of plume magmatic activity occurred after the Jalal hyperchron, the large interval of a stable geomagnetic polarity near the Mesozoic/Cenozoic boundary [Larson and Olson, 1991; and others]. Yet this assumption was not further elaborated. There is a time lag between processes at the Earth’s surface, affecting the evolution of life, magmatic activity, and so on, and processes in the liquid core, affecting the geomagnetic field behavior. Thus, the delay of the beginning of geological eras relative to reversal frequency minimums is noted for the Phanerozoic [Molostovskii et al., 1976; Pechersky and Didenko, 1995;

Khramov et al., 1982] and the entire Neogaea [Pechersky, 1997, 1998]. A similar lag behind reversal frequency extrema is characteristic of average velocity extrema of continents [Pechersky, 1998] and plume magmatic activity at the present time, near the Mesozoic/Cenozoic (Mz/Cz) boundary (the North Atlantic province and Deccan traps), and near the Paleozoic/Mesozoic (Pz/Mz) boundary (Siberian traps) with respect to their origination time established from the behavior of the geomagnetic direction variation amplitudes [Pechersky, 2001, 2006; Pechersky and Garbuzenko, 2005]. This delay is 20–60 Myr, implying that a plume rises from the core–mantle boundary to the Earth’s surface at a velocity of 4–10 cm/yr. Such a velocity is in agreement with the evaluations of the mean drift velocities of major continental plates [Pechersky, 1997, 1998; Zonenshain et al., 1987; Jurdy et al., 1995].

The present paper generalizes data on the behavior of such characteristics of the geomagnetic field as the amplitude of variations in the field direction, paleointensity, and the reversal frequency near the Pz/Mz and Mz/Cz boundaries and elucidates their relation to lower mantle plumes, namely, Deccan and Siberian traps and basalts of the North Atlantic province (the Greenland plume). We hope that the approach to spatiotemporal comparison proposed in this paper proves helpful for eliminating the uncertainty in the interpretation mentioned above.

#### VARIATIONS IN THE GEOMAGNETIC FIELD DIRECTION

The total amplitude of variations in the geomagnetic field direction can be determined from the angular standard deviation  $S = 81/K^{1/2}$ , where  $K$  is the precision parameter of individual vectors in statistics on a sphere [Khramov et al., 1982]. Thus, the value  $S$  is determined for the entire Neogaea [Pechersky, 1998]. The bulk of data on the amplitudes of spatiotemporal variations in the field direction is sufficient for the analysis of not only the global behavior of this characteristic but also local patterns related, in particular, to plume epicenters.

Now, we consider the behavior of  $S$  near the Pz/Mz and Mz/Cz boundaries, using the GPMDB-2005 database of paleomagnetic data. Paleomagnetic determinations in the intervals 340–200 and 140–35 Ma were chosen from the database. This choice was based on the following considerations. (a) The main pulses of active surface magmatism near the Mz/Cz and Pz/Mz boundaries are associated with three large plumes; the latter are the ~55 Ma Greenland plume (basalts of the North Atlantic province), the 65 Ma Deccan plume [Grachev, 2000; Courtillot et al., 2003], and the 251 Ma Siberian plume (less intense magmatic activity encompasses the interval 22–26 Ma [Ivanov et al., 2005] and no less than six magnetic chrons of normal and reversed polarities [Gurevich et al., 2004]). Taking into account rather large intervals of paleomagnetic age determinations, the 20–30 Myr following the completion of trappean magmatism were included in the comparison in order to gain deeper insights into geomagnetic field variations. (b) Earlier, based on the example of recent plume magmatism, it was shown [Pechersky, 2001] that the  $S$  value and its scatter increase toward the plume epicenter, and this increase is noticeable over the 40–50 Myr before the beginning of active plume magmatism at the Earth's surface, reflecting the time of activity near the core–mantle boundary, which led to an increase in the variation amplitude of the geomagnetic field and the plume formation. (c) If such phenomena as impacts of asteroids near the boundaries of geological eras affected the  $S$  behavior, we took them into account by considering intervals overlapping the Pz/Mz and Mz/Cz boundaries, i.e., including times before, during, and after the periods of noticeable asteroid impacts.

In the chosen interval of paleomagnetic age determinations, the age data were classified according to the following four categories.

(1) **Unreliable paleomagnetic data.** The number of samples used for a determination is no more than ten, thermal demagnetization is either absent or heating temperatures do not exceed 200°C, the AF demagnetization field is no more than 15 mT, the precision parameter is less than 7, the confidence angle  $\alpha_{95}$  exceeds 25°, and the coordinates of the paleopole differ sharply from the coordinates of the mean pole of this time for a given continent (paleomagnetic determinations reflect an overprinting of more ancient rocks). Such determinations were excluded from further consideration.

(2) **Low reliability of paleomagnetic determinations.** The number of samples is no more than 20, thermal demagnetization temperatures are not higher than 400°C, and the AF demagnetization field is not higher than 30 mT. The index of paleomagnetic reliability of this group of determinations is accepted to be equal to 0.1, and this value is used as a weight in calculations of average  $S$  values.

(3) **Intermediate reliability of paleomagnetic determinations.** The number of samples is more than 20, thermal demagnetization temperatures are not lower than 500°C, the AF demagnetization field is not less than 50 mT, and some field tests (fold, conglomerate, baking, and reversal) are positive. The index of paleomagnetic reliability is 0.5, and this value is used as a weight in calculations of average  $S$  values.

(4) **High reliability of paleomagnetic determinations.** The number of samples is more than 20, comprehensive thermal and AF demagnetizations are carried out with the relevant component analysis and extraction of the characteristic component of natural remanent magnetization (NRM), and no less than two field tests (fold, conglomerate, baking, and reversal) are positive. An index of paleomagnetic reliability of 1.0 is used as a weight in calculations of average  $S$  values. We should emphasize that the field tests of paleomagnetic reliability such as the fold, conglomerate, reversal, and baking tests are important only for establishing the primary NRM component and this is by no means decisive evidence for the adequacy of a determined  $S$  value to the total amplitude of variations in the geomagnetic field direction. As is shown below, the scatter in  $S$  values is very significant, primarily due to technical and methodological factors (inadequate demagnetization, measurement uncertainties, magnetic bias during demagnetization, a large interval of age involved in the calculation of the average paleomagnetic direction, and so on). Therefore, only mean and modal  $S$  values can be considered, to an extent, as reliable.

The paleomagnetic determinations that remained after rejection were subdivided into the following age intervals: 340–315, 310–290, 285–270, 265–245, 240–200, 145–112, 110–95, 94–83, 82–73, 72–63, 62–50, and 45–25 Ma. In age intervals within the range 340–

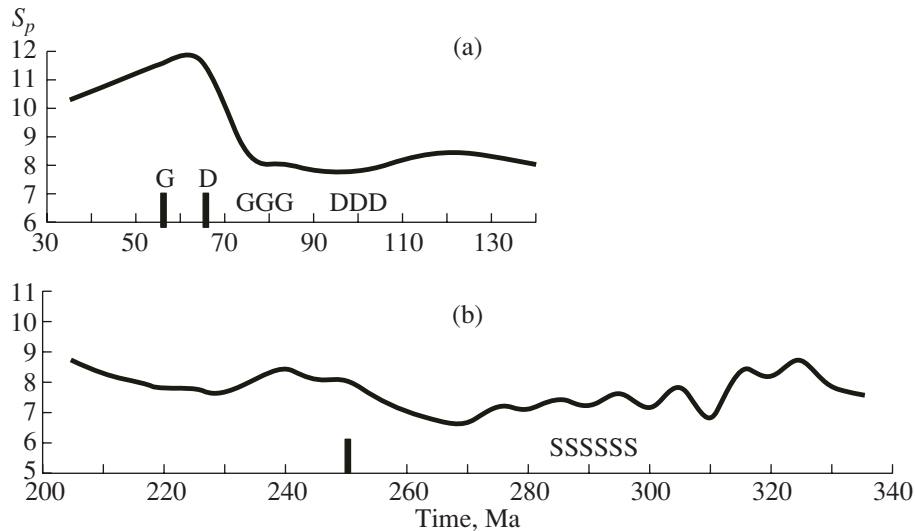


**Fig. 1.** Total amplitude of variations in the geomagnetic field direction  $S_p$  near the Mz/Cz (a) and Pz/Mz (b) boundaries (an averaging window of 10 Myr). The times of surface magmatic activity of the Greenland, Deccan (the Mz/Cz boundary), and Siberian (Pz/Mz) plumes are indicated by solid vertical bars at the time axis, and the formation times of the Greenland, Deccan, and Siberian plumes near the core–mantle boundary (reconstructions made in this work from paleomagnetic data) are indicated by the bold letters G, D, and S, respectively.

200 Ma, we used maps of paleotectonic reconstructions and apparent polar wander paths (APWPs) for all continents [Torsvik and Van der Voo, 2002; Scotese and McKerron, 1990; Pechersky and Didenko, 1995; Bretstein and Klimova, 2005; McElhinny and McFadden, 2000; Smethurst et al., 1998]. In age intervals within the range 145–25 Ma, maps of geodynamic reconstructions obtained with the help of the plate tectonic reconstruction service (ODSP) program were used.

Paleomagnetic determinations were plotted as points in paleotectonic reconstruction maps, which yielded their ancient coordinates. For the Pz–Mz interval, two models of paleotectonic reconstructions exist, one with a dipole geomagnetic field (the GAD model) and another including a nondipole (octupole) component (the G3 model) [Torsvik and Van der Voo, 2002]. Without analyzing the validity of these models, we determined the ancient coordinates of paleomagnetic observation points in both models. For each paleomagnetic determination, the angular distance along a great circle to the epicenters of three plumes was measured: the Deccan traps with the reconstructed 65 Ma center (50°E, 20°S); basalts of the North Atlantic province, 55 Ma (30°E, 60°E); and Siberian traps, 250 Ma ((57°N, 30°E) according to GAD and (60°N, 45°E) according to G3). In the latter case, two variants of great circle angular distances from each paleomagnetic determination point to the center of Siberian traps were determined. We assumed that the position of plume epicenters did not vary noticeably throughout the period under study.

The difference between distance estimates from the two models is generally no more than 10°, a value insignificant for our task; only for distances of more

than 80° does the difference occasionally reach 20° or more in areas where the Siberian plume was most likely unrelated to the variations [Pechersky, 2006]. Therefore, only the G3 model is considered below.

In determining the coordinates of a paleomagnetic observation point, two factors were considered: the paleolatitude determined from the paleomagnetic inclination of this point and the position of the latter in the map of paleoreconstruction of the corresponding age according to various geographic attributes such as the position relative to river bends, bank outlines, and so on. The point is that, in many cases, rather wide ranges are indicated in the database for rock ages and paleomagnetic determinations. Therefore, we chose such a map that the position of a point agreed best with its paleolatitude determined from the paleomagnetic inclination. The correspondence of the polarity of this paleomagnetic determination to the geomagnetic polarity timescale [A Geological ..., 2004] within a 5-Myr averaging interval was also taken into account.

The  $S$  value depends on the latitude:  $S$  smoothly decreases by about two times from the equator to the pole. This dependence is valid for steady state intervals of the geomagnetic field throughout the Neogaea [Pechersky, 1996]. Using the latitude dependence of  $S$ , all determinations of  $S$  are reduced to one paleolatitude, the pole latitude  $S_p$ .

Depending on the model accepted (GAD or G3), the paleolatitudes of observation points are somewhat different; accordingly, the  $S_p$  values reduced to one latitude will also differ. In the vast majority of cases, this difference between  $S_p$  values as determined from both models does not exceed 1°–2° [Pechersky, 2006].

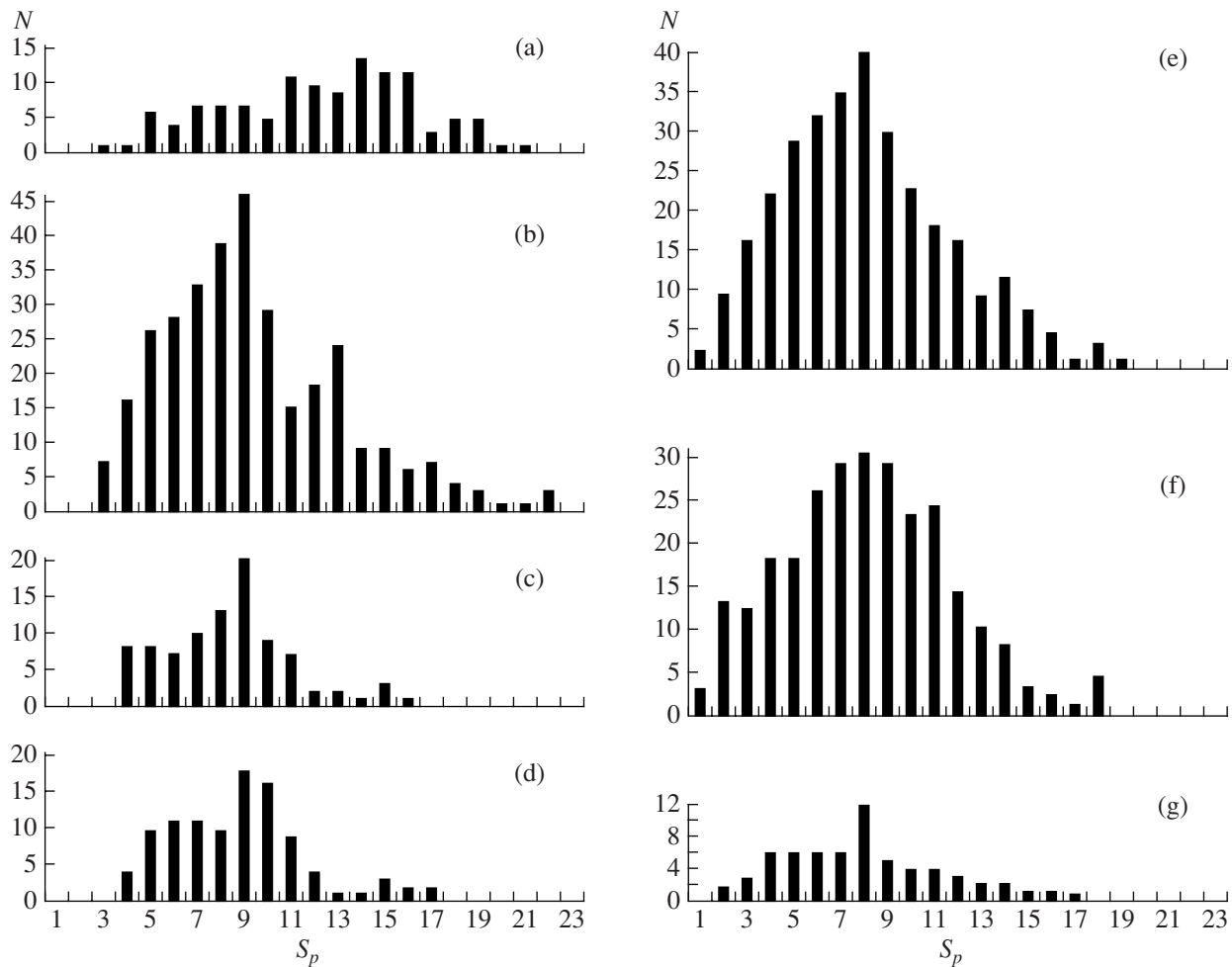


**Fig. 2.** Histograms of amplitudes of variations in the geomagnetic field direction  $S_p$ : (a, b) volcanic rocks and sediments; (c) intrusions; (d) volcanic rocks and sediments occurring at a distance from plume epicenters of more than  $60^\circ$ ; (e–g) predominantly sediments (+ volcanic rocks). The rock ages are (a) 65–25, (b–d) 140–75, (e) 265–200, (f) 270–310, and (g) 335–315 Ma.

The selected paleomagnetic determinations are distributed over intervals of 5–10 Myr and, for each interval, the weighted mean was calculated and smoothing with a 10 Myr window was carried out (Fig. 1). The resulting plot characterizes the behavior of the direction variation amplitude for the “normal” geomagnetic field, with scatters of various origins being smoothed. As seen from the figure, the direction variation amplitude of the normal field is lowest ( $7^\circ$ – $8^\circ$ ) during the steady state periods of the geomagnetic field, namely, in the Kiama (296–266 Ma) and Jalal (115–85 Ma) hyperchrons. Later,  $S_p$  increases up to  $9^\circ$  at Pz/Mz and up to  $12^\circ$  at Mz/Cz. The Pz/Mz and Mz/Cz boundaries lie within intervals of an increase in the  $S_p$  average near its maximum. Both boundaries of the geological eras do not exhibit any well-expressed features of  $S_p$ .

The global pattern of the direction variation amplitude is reflected in the histograms of the  $S_p$  distribution (Fig. 2). Here, the main distribution modes  $9^\circ$  (Mz/Cz, Figs. 2b–2d) and  $8^\circ$  (Pz/Mz, Figs. 2e–2g) are well recognizable. In accordance with a noticeable global

increase in the variation amplitude in the interval 65–35 Ma, the  $S_p$  mode in this interval is equal to  $14^\circ$  (Fig. 2a). Against the main distribution, a second group of higher values of  $S_p$  with the modes  $13^\circ$  (Fig. 2b) and  $11^\circ$  (Fig. 2f) is distinguishable. In the histogram for intrusions, the first mode of  $S_p$  is clearly observed, but the second mode with  $S_p = 12^\circ$ – $13^\circ$  is absent (Fig. 2c), implying a short-term source of the second mode [Pechersky and Garbuzenko, 2005; Pechersky, 2006].

Now, we address the dependence of  $S_p$  on the distance between a paleomagnetic observation point and the epicenter of the nearest of the plumes specified above. We should emphasize that the distance between the plume epicenter and its origination place at the core–mantle boundary is about 3000 km and the rise path of a plume can be inclined [Ernst and Buchan, 2003]. Accordingly, given the aforementioned uncertainty in the distance to the plume generation place and an unsteady state at the core–mantle boundary matched by an unsteady state of the geomagnetic field, an

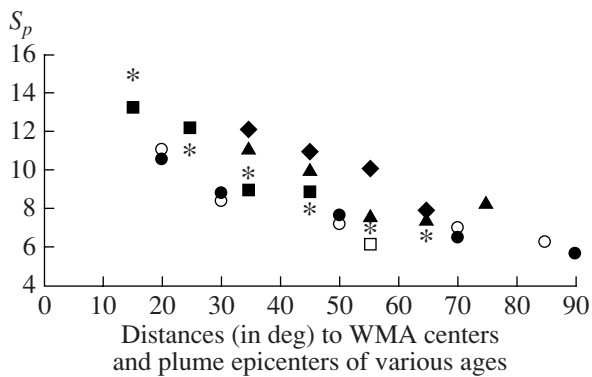


**Fig. 3.** Distribution of  $S_p$  as a function of distance to centers of contemporary world magnetic anomalies (WMAs) and plume epicenters in the degrees of great circle arcs: world magnetic anomalies (asterisks); contemporary plumes (solid squares), the paleomagnetic record age is 45–40 Ma [Pechersky, 2001]; unreliable determination from two points (open square); Greenland plume, North Atlantic province (solid diamonds), the paleomagnetic record age is 82–73 Ma [Pechersky and Garbuzenko, 2005]; Deccan plume (solid triangles), the paleomagnetic record age is 110–95 Ma [Pechersky and Garbuzenko, 2005]; Siberian plume (open circles), the paleomagnetic record age is 285–270 Ma; Siberian plume (solid circles), the paleomagnetic record age is 300–290 Ma. The  $S_p$  values are averaged over ten-degree intervals.

approach toward the plume epicenter should be accompanied by an increase in the variation amplitude (i.e.,  $S_p$ ) and an increase in the scatter of  $S_p$  values. Moreover, the distribution of  $S_p$  relative to the epicenters of the selected plumes can be noticeably disturbed by the presence of other plumes of various ages that were active at the time under consideration. In addition to the causes mentioned above, one should take into account technical uncertainties involved in measurements, the identification of the primary NRM component (the presence of stable secondary components), and so on. All of them increase the scatter in individual values of  $S_p$ , and only mean values and modes are more reliable quantitative characteristics. Accordingly, the values of  $S_p$  averaged over ten-degree intervals of distances were calculated for the analysis of the behavior as a function of the distance to plume epicenters (Fig. 3).

The situation near the Mz/Cz boundary can be characterized as follows [Pechersky and Garbuzenko, 2005].

**~(110–95) Ma.** In the Deccan case, the scatter in  $S_p$  values begins to be appreciable at a distance of more than  $100^\circ$  and reaches  $3^\circ$ – $16^\circ$  on approaching the plume. The weighted  $S_p$  average increases up to the second mode value  $11.5^\circ$  toward the plume epicenter (Figs. 2b, 3). In the case of the Greenland plume, such a tendency is virtually absent, as is evident from the weighted average of  $S_p$ , which corresponds to the normal field level at this time (Fig. 1).

**~(94–83) Ma.** The weighted averages of  $S_p$  for both plumes are at the level of the normal field and first mode (Figs. 1, 2b, 2d, 3), and the scatter in amplitudes is large ( $2^\circ$  to  $17^\circ$ ).

**~(82–73) Ma.** In the case of the Deccan plume, the dependence on the distance to the plume epicenter is not observed. The values of  $S_p$  lie within the range  $3^\circ$ – $15^\circ$ , and the weighted average ( $9^\circ$ ) lies within the first mode (Fig. 1). A different pattern is observed in the case of the Greenland plume: far from this plume, the level of  $S_p$  corresponds to the first mode (the average is  $S_p = 8.4^\circ$ ) (Fig. 3). The weighted average of  $S_p$  increases toward the plume up to  $12^\circ$  (Fig. 3, the second mode in Fig. 2b) and the scatter in  $S_p$  values varies from  $2^\circ$  to  $22^\circ$ .

**~(72–25) Ma.** This interval is characterized by a large scatter of  $S_p$  values (from  $3^\circ$  to  $20^\circ$ ) regardless of the distance to the plumes. The mode  $13^\circ$ – $14^\circ$  corresponds to a noticeable increase in the normal field level (Fig. 1).

The situation near the Pz/Mz boundary is as follows [Pechersky, 2006].

**340–315 Ma.** The  $S_p$  distribution is dominated by low values ( $4^\circ$ – $8^\circ$ ) with a mode of  $8^\circ$  (Fig. 2g). In this time interval, the latter corresponds to the normal field (Fig. 1).

**310–290 Ma.** The distribution of  $S_p$  values has two modes (Fig. 2f). The first mode ( $7^\circ$ ) corresponds to the normal field of this time interval (Fig. 1). The second mode ( $11^\circ$ ) depends on the distance to the center of Siberian traps, as is evident from averages of  $S_p$  (Fig. 3).

**285–270 Ma.** The distribution of  $S_p$  is bimodal (Fig. 2f). The first mode  $8^\circ$  relates to the normal field, and the second mode  $11^\circ$  is associated with an increase in  $S_p$  toward the center of Siberian traps (Fig. 3).

**265–245 and 240–200 Ma.** This time is characterized by a single-mode distribution of  $S_p$ . Its mode is  $8^\circ$ , which corresponds to the normal field (Fig. 1).

## RESULTS AND DISCUSSION

The bimodal distributions of  $S_p$  within the time intervals 300–270 and 140–75 Ma are due to two factors.

(a) **Global factor.** The first mode of  $S_p$  exists throughout the time intervals under consideration and does not depend on the distance to a plume epicenter (Fig. 2).

(b) **Local factor.** The second, higher mode of  $S_p$  exists only at relatively short distances from plume epicenters (Figs. 2, 3) and vanishes at greater distances, which is clearly seen from the histogram (Fig. 2) and is confirmed by  $S_p$  averages (Fig. 3). Consequently, during the time under consideration, the amplitude of variations in the geomagnetic field direction averaged  $7^\circ$ –

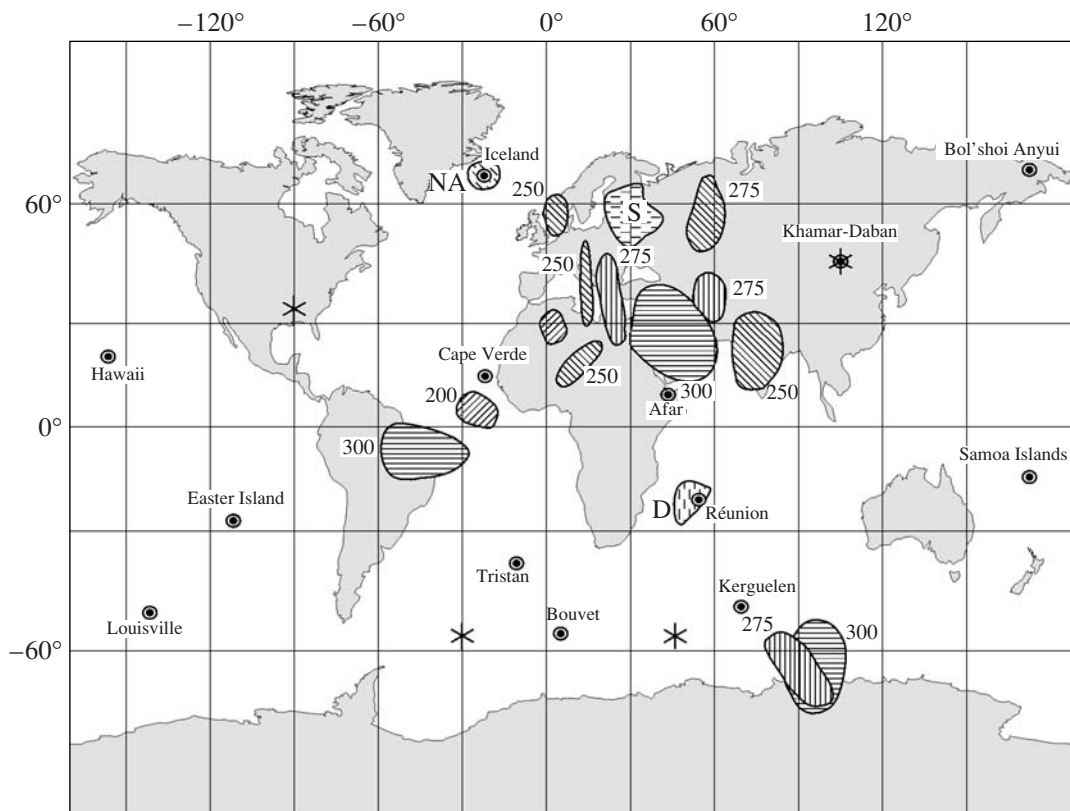


**Fig. 4.** Map showing the occurrence areas of compact groups of higher amplitudes of variations in the geomagnetic field direction ( $S_p \geq 9^\circ$ ) of various ages (shaded areas with age intervals shown near their contours). Also shown are epicenters of contemporary plumes (double circles), centers of world magnetic anomalies (asterisks), fields of (D) Deccan traps and (NA) the North Atlantic volcanic province (65 Ma paleoreconstruction), and (S) Siberian traps (250 Ma paleoreconstruction).

$8^\circ$  (Fig. 1). This global effect, characterizing the normal state of the geomagnetic field of predominantly normal or reversed polarity, is superimposed by an anomalous field state of a local origin. Evidently, it was caused by intense disturbances in the normal state of the geomagnetic field and by plume origination during this time.

A decrease in the second mode of  $S_p$  along the succession volcanics–sediments–intrusions noted in [Pechersky and Garbuzenko, 2005] is most likely associated with the remanence acquisition time interval (the mode is maximal in volcanics, acquiring the NRM almost instantaneously, and vanishes in intrusions with a significantly extended time of NRM acquisition), indicates a short lifetime of high-amplitude anomalous variations, and relates to short time intervals of an unsteady state of the geomagnetic field caused by local disturbances at the core–mantle boundary that lead to the plume formation. The local factor and its short-term effect are confirmed by the absence of the second mode of  $S_p$  far from plume epicenters (Fig. 2d) and in the histogram of intrusions (Fig. 2c).

A large scatter of  $S_p$  values near plume epicenters is additional evidence for a relatively short lifetime of high amplitude variations because  $S_p$  values spaced at approximately 10 Myr fall in each time interval under

consideration. The following fact also supports the short lifetime of the anomalous amplitudes of magnetic field variations and plume formation times. The variation amplitude rises toward contemporary world magnetic anomalies (Fig. 3), and the lifetime of the world anomalies is less than 20 kyr [Pechersky, 2000, 2001]. This suggests a close relationship between the sources of world magnetic anomalies and plume formation and short times of both phenomena. The short time length of the main activity pulse of Siberian traps is in agreement with this assumption. On the other hand, the activity of the Iceland (Greenland) plume (the North Atlantic volcanic province); the Réunion plume (Deccan traps); or such plumes as the Hawaiian, Kerguelen (Raj Mahal traps), Tristan (Parana traps), and others, encompasses a period of  $\sim 100$  Myr [Courillot et al., 2003; Ernst and Buchan, 2003]. This implies that a disturbance at the core–mantle boundary responsible for the increase in the field variation amplitude and for the plume formation rapidly decays in the core, but the resulting “source” at the mantle base can exist for a hundred million years, similar to magma chambers in the crust, where large intrusive bodies cool over millions of years. Finally, the mismatch between the short lifetimes of world magnetic anomalies and main activity pulses of plume magmatism at the Earth’s surface,

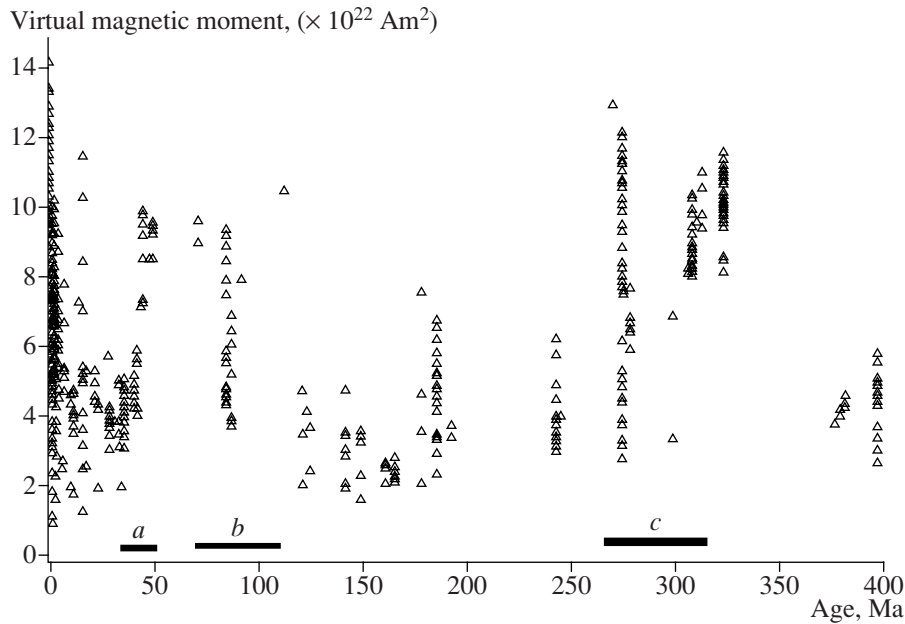


**Fig. 5.** Variation in the virtual magnetic moment in the interval 0–400 Ma [Shcherbakov et al., 2002]. The horizontal bars near the age axis are intervals of plume formation near the core–mantle boundary: (a) contemporary plumes; (b) Greenland and Deccan superplumes; (c) Siberian superplume.

on the one hand, and the long time interval of noticeable plume influence on the field variation amplitude, on the other hand, can be attributed to the fact that short activity pulses in the core occurred repeatedly within the time interval under consideration and they resulted in the formation of systems of plumes, namely, superplumes, but not all of the latter reached the Earth's surface.

The delay of surface magmatism with respect to an excited state of the core that caused an increase in the field variation amplitude and plume formation is 20–50 Myr for magmatic activity of both contemporary plumes and those confined to the Mz/Cz and Pz/Mz boundaries [Pechersky, 2001, 2006; Pechersky and Garbuzenko, 2005]. Such an extended delay interval can be accounted for by two alternative factors. The first, **trivial** factor is that this is a result of uncertainties in rock datings and paleomagnetic determinations; the related average delay time is 35 Myr. The second, **non-trivial** factor is that large events associated with the Deccan traps, Siberian traps, and North Atlantic volcanic province might have been due to repeated pulses of core activity that resulted in the formation of the Siberian, Deccan, and other superplumes [Ernst and Buchan, 2003]. The rise time of plumes was theoretically estimated at 0.5–3 Myr [Dobretsov et al., 2001], implying rise velocities 10 to 40 times higher than our estimate. With this rise time, an increase in  $S_p$  values toward the plume epicenter should be almost synchronous with the arrival time of a plume at the Earth's surface. However, this phenomenon is not observed in relation to contemporary or more ancient plumes.

Apart from the increase in  $S_p$  values noted within the time interval 300–270 Ma, increased values of  $S_p$  are recorded far from the center of Siberian traps in all time intervals considered. These are, first, randomly distributed points possibly related to uncertainties involved in estimation of the precision parameter for paleomagnetic directions and, second, higher values of  $S_p$  forming compact groups (Fig. 4). Evidently, such compact groups are regions of excited states of the Earth's core near its boundary with the mantle, i.e., origination zones of lower mantle plumes whose arrival at the Earth's surface “is expected” 20–50 Myr after the formation time of the corresponding groups. Some such groups, located to the south of the occurrence area of Siberian traps, are possible formation regions of the Siberian superplume, whose rise was not strictly vertical but deviated to the north. It is noteworthy that regions of plume formation spread from older (310–290 Ma) to younger (280–270 and 260–240 Ma) ones in both eastward and westward directions (Fig. 4).

The considered Carboniferous–Triassic interval includes the existence of the Pangea supercontinent, on the territory of which paleomagnetic observation points are distributed rather uniformly. Unfortunately, the Mesozoic–Cenozoic interval cannot be considered in a similar way because, at this time, the majority of Cretaceous–Paleogene rocks are distributed nonuniformly along the Alpine and Pacific belts. Therefore, it is virtually impossible to gain constraints on the presence of compact areas of higher amplitudes of variations in the magnetic field. The centers of contemporary world magnetic anomalies, epicenters of several contempo-

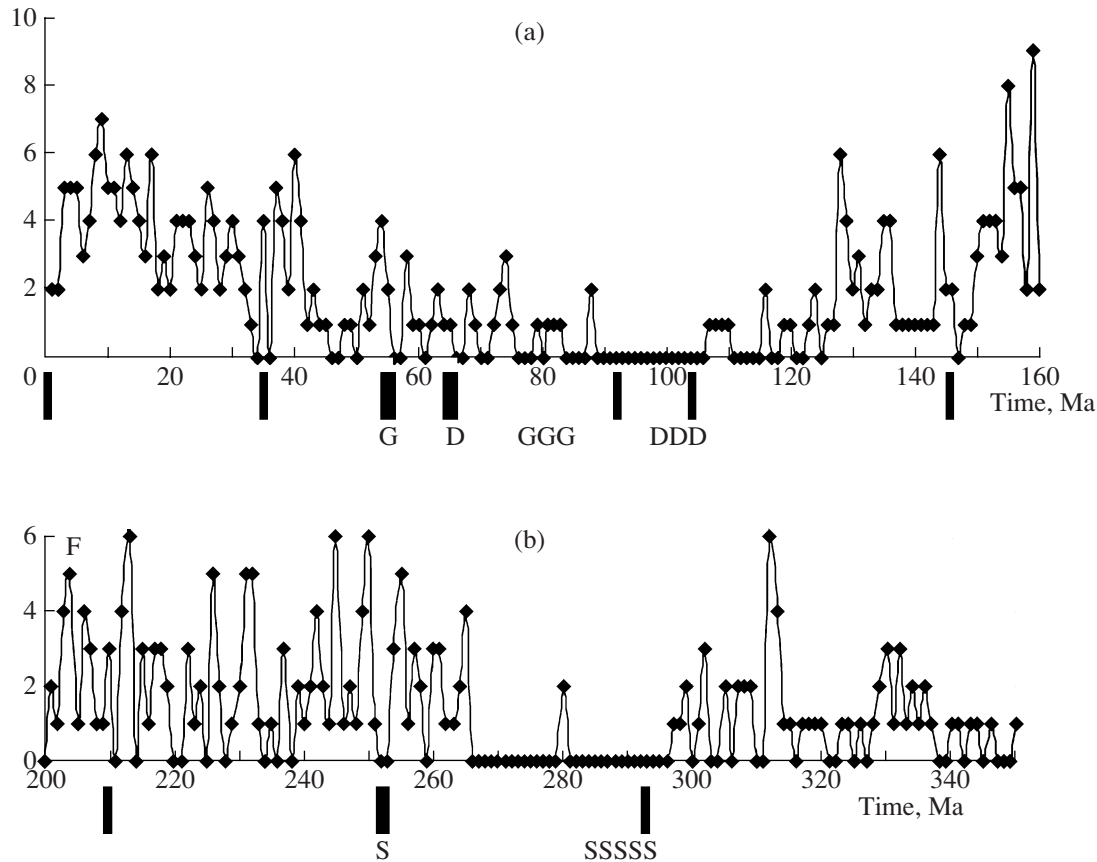


**Fig. 6.** Reversal frequency (the number of reversals per 1 Myr) in the intervals (a) 0–160 and (b) 200–350 Ma. The plots are constructed on the basis of the polarity timescale presented in [A Geological ..., 2004] and refined in [Molostovskii et al., 2004]. The times of surface magmatic activity of the most reliable lower mantle plumes [Grachev, 2000; Ernst and Buchan, 2003] are indicated by vertical bars below the time axis; the thick vertical bars with letters below the time axis indicate the formation times of the Greenland (G), Deccan (D), and Siberian (S) plumes near the core–mantle boundary (reconstructions made in this work from paleomagnetic data) and the times of their arrival at the Earth's surface.

rary plumes, and epicenters of the Greenland, Deccan, and Siberian plumes [Grachev, 2000; Courtillot et al., 2003] are plotted in Fig. 4. It is evident that some of them are very close to each other: the Tristan and West Antarctic anomalies; the Kerguelen and East Antarctic anomalies and the possible Permo-Carboniferous plume southeast of Kerguelen; Afar and the possible region of the Siberian superplume; and the contemporary plume of the Cape Verde Islands, from which a 200- and 300-Ma chain extends to the southwest (possible activity traces of a single plume). Moreover, some features coincide; these are the Iceland and Greenland plumes, Réunion and Deccan plumes, Asian anomaly and Khamar-Daban plume, and Kerguelen and Raj Mahal. However, some of the plume epicenters are widely spaced. First of all, these are plumes of the Pacific Ocean, where paleomagnetic determinations are almost absent (Fig. 4). This leads to the following conclusions. (1) Except the Triassic–Permian–Carboniferous system of plumes, with which the Siberian superplume is probably associated, the remaining plumes are scattered rather chaotically over the surface of the

Earth's core. (2) Both short- and long-lived plumes have been revealed. These are primarily the system of plumes (a superplume) existing from the Carboniferous up to the present (Afar?); the Greenland plume, existing from about 80 Ma up to the present (Iceland); the Deccan plume, which formed about 100 Myr ago and exists at present (Réunion); the plume near Kerguelen, formed in the Carboniferous; the Raj Mahal plume, the presently existing Kerguelen plume; the East Antarctic anomaly; and, finally, the Khamar-Daban plume, existing from about 50 Ma up to the present (the Asian magnetic anomaly). Some plumes existing for a long time ascended strictly vertically (Khamar-Daban, Deccan, and Kerguelen), while others deviated noticeably from the vertical (the West Antarctic anomaly–Tristan, the East Antarctic anomaly–Kerguelen–southern plume, and the system of Permo–Carboniferous plumes–Afar?). Long-term existence of plumes does not indicate their continuous activity: judging from the above data and considerations, this is a series of short-term activity pulses in a large region at the core–mantle boundary.

## PALEOINTENSITY

Data of determinations of the paleointensity by heating methods (primarily the Thellier technique) and the dipole magnetic moment calculated from the paleointensity are assembled in databases and are generalized in [Pechersky, 1998; Shcherbakov et al., 2002].

According to these data (Fig. 5), beginning from ~80 Ma, i.e., 15–20 Myr prior to the Mz/Cz boundary, the paleointensity rather sharply increased (by about two times) and remained at this level up to 45 Ma, when it again abruptly dropped by a factor of 2. The pattern near the Pz/Mz boundary is different. Here, the paleointensity was higher in the interval 330–280 Ma, after which it dropped, on average, by about two times 30 Myr prior to the Pz/Mz boundary and remained at this level up to 200 Ma. Magmatic activity peaks of Deccan and Siberian traps are confined to the Mz/Cz and Pz/Mz boundaries (65 and 251 Ma), i.e., lie within the range of high and low paleointensities, respectively (Fig. 5). If we consider not values of the paleointensity but its variations, i.e., the ratio of the standard deviation of the paleointensity to its average for each 10 Myr interval [Pechersky, 1997, 1998], variation features specific to the era boundaries are not observed in this case either. Thus, no relationship exists between the paleomagnetic intensity and the boundaries of geological eras along with maximums of magmatic activity of the Deccan and Siberian traps. Moreover, they are confined to paleointensity differing by two times. Addressing the formation times of plumes at the core–mantle boundary, we see that all these times are marked by significant changes in the paleointensity: the recent plumes originated in the 50–40-Ma interval, when the paleointensity dropped by more than two times; the Greenland and Deccan plumes originated in the ~100–80-Ma interval, when the paleointensity was higher by about two times; and the origination of the Siberian plume in the interval ~310–275 Ma was associated with an approximately twofold drop in the paleointensity (Fig. 5).

## GEOMAGNETIC POLARITY AND REVERSAL FREQUENCY

We analyzed the polarity and the reversal frequency of the magnetic field, using the timescale of the geomagnetic polarity published in [A *Geological ...*, 2004] with refinements and supplements by E.A. Molostovskii, A.Yu. Guzhikov, and others. Based on this scale, plots of the geomagnetic reversal frequency (the number of reversals per 1 Myr) were constructed (Fig. 6). As seen from the figure, the Mz/Cz and Pz/Mz boundaries, i.e., the times of the most intense changes in biota and the highest activity of Deccan and Siberian traps, coincide with intervals of frequent reversals and, accordingly, frequent polarity changes, which is not reflected in these characteristics of the geomagnetic field. The transition from the stable

regime of absence of reversals to the regime of frequent polarity changes occurs ~15 Myr prior to both boundaries. We should emphasize that, although no correlation exists between the reversal frequency and the paleointensity, the reversal frequency correlates with variations in the paleointensity ( $dH/H$ ). Thus, with the averaging of data in the 10 Myr interval, the main extrema of the reversal frequency and the paleointensity variation coincide in time: 100, 200, 290, and 310 Ma (minimums) and 60–50, 140, 240, and 330 Ma (maximums) [Pechersky, 1997, 1998]. Consequently, variations in the two basic characteristics of the geomagnetic field, which reflect processes in the liquid core, appear to be synchronous (but this does not hold for their values!), and a relation between paleointensity variations and plume formation is observed, although such a relation is absent for the reversal frequency: the plume formation times are associated with very diverse variants of the frequency of reversals, from their absence to maximum values. The times of high magmatic activity of plumes at the Earth's surface are marked in Fig. 6. As shown above, plumes formed at the core–mantle boundary 20–50 Myr earlier.

Accordingly, if the surface plume activity times are shifted back by these 20–50 Myr, the resulting times of plume formation will lie in intervals of very diverse reversal frequency values. This is evidence of the absence of a relation between the processes of geomagnetic reversals and plume formation.

## CONCLUSIONS

Generalization of data on the amplitude of variations in the geomagnetic field direction, paleointensity, and reversal frequency over the last 50 Myr near the Paleozoic–Mesozoic and Mesozoic–Cenozoic boundaries, with which magmatic activity peaks of Siberian and Deccan traps coincide [Pechersky, 2001, 2006; Pechersky and Garbuzenko, 2005], revealed the following regular pattern: the boundaries of geological eras have no signatures in records of the paleointensity, polarity, reversal frequency, or variations in the geomagnetic field direction. The boundaries of eras lie in intervals of frequent polarity changes 15–20 Myr after the preceding hyperchrons of the steady state single-polarity field. Against the background of the normal field, there is observed an almost invariable tendency of an increase in the field direction variation amplitude toward the epicenters of recent lower mantle plumes; the Greenland, Deccan and Siberian superplumes; and world magnetic anomalies. Certain differences in the  $S_p$  variation level changes toward epicenters of plumes and world magnetic anomalies (Fig. 3) are due to global temporal changes in the normal field. The above is evidence for a common origin of the onset of lower mantle plumes of different formation times, world magnetic anomalies, and rises in the amplitude of geomagnetic direction variations; i.e., all these phenomena are

results of a local excitation in the upper part of the liquid core.

The origination of superplumes is confined to intervals of large changes in the paleointensity (drops or rises). On the other hand, plume generation processes and the reversal frequency are uncorrelated: the plume formation times are associated with very diverse variants of the frequency of reversals, from their total absence to maximum values. Evidently, this fact indicates *different sources of world magnetic anomalies, variations in the field direction and paleointensity, and plumes, on the one hand, and geomagnetic reversals, on the other.* While sources of the first group of phenomena are confined to the core–mantle boundary, one may suppose that reversals are generated near the liquid–solid core boundary. This resembles the state of an ocean: storms at its surface do not reach its floor and events at the ocean floor are observed at the surface only as weak responses. Thus, the amplitude of variations in the magnetic field direction within hyperchrons of a steady state of the geomagnetic field (with a predominant single polarity) is lower than during periods of its unsteady state (frequent reversals). This is a global phenomenon. The same can be said in relation to the magnetic field value: its variations correlate with the reversal frequency (this is also a global phenomenon), and they are related to local disturbances near the core–mantle boundary that lead to both an increase in the amplitude of magnetic field variations and plume formation.

The “delay” of magmatic activity of a plume at the Earth’s surface with respect to its origination at the core–mantle boundary is the rise time interval of the plume. In all cases considered in this work, this time is within the limits 20–50 Myr. Apparently, the differences in the plume rise times are related to different rise paths, slowdowns of the plume movement, and so on. The spread of the “delay” time may be accounted for by an uncertainty in datings of paleomagnetic study objects and/or the NRM, but it is more likely that this is due to the formation, within the time interval considered, of a series of plumes (superplumes) approximately in the same region at the core–mantle boundary. This interpretation is supported by the existence of compact clusters of higher amplitudes of the magnetic field direction in the interval 300–200 Ma (these clusters delineate possible regions of formation of world magnetic anomalies and plumes). The region of activity in the upper part of the Earth’s core located to the south of the occurrence area of Siberian traps may be associated with the formation of a series of plumes (the Siberian superplume) ascending along different paths that were not strictly vertical but deviated to the north; moreover, not all of the plumes reached the Earth’s surface. Since the activity region of the Siberian superplume includes the contemporary Afar plume, its (their) activity encompasses the time from the Carboniferous to the present. Long-term activity is also typical of such plumes as the Iceland–Greenland, Réunion–Deccan,

Kerguelen–Raj Mahal, Khamar-Daban, Hawaiian, and other plumes.

#### ACKNOWLEDGMENTS

I am grateful to V. Vodovozov for help in preparing computer graphics. This work was supported by the program “Lower Mantle Plumes and Geodynamics of the Lithosphere” of the Division of Earth Sciences, Russian Academy of Sciences.

#### REFERENCES

1. *A Geological Time Scale*, Ed. by F. M. Gradstein et al. (Univ. Press, Cambridge, 2004).
2. Yu. S. Bretstein and A. V. Klimova, “The Paleomagnetism of Phanerozoic Terranes, Far East Russia: Comparison with North-China Plate Data (Review),” *Russ. J. Earth Sci.* **7** (1) (2005); <http://rjes.wdcb.ru>.
3. V. Courtillot, A. Davaille, J. Besse, and J. Stock, “Three Distinct Types of Hotspots in Earth’s Mantle,” *Earth Planet. Sci. Lett.* **205**, 295–308 (2003).
4. N. L. Dobretsov, A. G. Kirdyashkin, and A. A. Kirdyashkin, *Deep Geodynamics* (SO RAN, Novosibirsk, 2001) [in Russian].
5. R. E. Ernst and K. L. Buchan, “Recognizing Mantle Plumes in the Geological Record,” *Annu. Rev. Earth Planet. Sci.* **31**, 469–523 (2003).
6. A. F. Grachev, “Mantle Plumes and Problems of Geodynamics,” *Fiz. Zemli*, No. 4, 3–37 (2000) [*Izvestiya, Phys. Solid Earth* **36**, 263–294 (2000)].
7. E. L. Gurevich, C. Heunemann, V. Radko, et al., “Paleomagnetism and Magnetostratigraphy of the Permian–Triassic Northwest Central Siberian Trap Basalts,” *Tectonophysics* **2**, 211–226 (2004).
8. A. V. Ivanov, S. V. Rasskazov, G. D. Feoktistov, et al., “ $^{40}\text{Ar}/^{39}\text{Ar}$  Dating of Usol’skii Sill in the South-Eastern Siberian Traps Large Igneous Province: Evidence for Long-Lived Magmatism,” *Terra Nova*, 1–6 (2005).
9. D. M. Jurdy, M. Stefanick, and C. R. Scottese, “Paleozoic Plate Dynamics,” *J. Geophys. Res.* **100**, 17965–17975 (1995).
10. A. N. Khramov, G. I. Goncharov, R. A. Komissarova, et al., *Paleomagnetology* (Nedra, Leningrad, 1982) [in Russian].
11. R. L. Larson and P. Olson, “Mantle Plumes Control Magnetic Reversal Frequency,” *Earth Planet. Sci. Lett.* **107**, 437–447 (1991).
12. M. W. McElhinny and P. L. McFadden, *Paleomagnetism. Continents and Oceans* (Academic, San Diego, 2000).
13. E. A. Molostovskii, M. A. Pevzner, D. M. Pechersky, et al., “Magnetostratigraphic Timescale of the Phanerozoic and the Geomagnetic Field Reversal Regime,” in *Geomagnetic Research* (Nauka, Moscow, 1976), Vol. 17, pp. 45–52 [in Russian].
14. D. M. Pechersky, “Latitude Dependence of the Total Amplitude of Paleovariations in the Geomagnetic Field Direction in the Neogaea,” *Geomagn. Aeron.* **36** (5), 130–136 (1996).

15. D. M. Pechersky, "Some Properties of the Geomagnetic Field over 1700 Million Years," *Fiz. Zemli*, No. 5, 3–20 (1997) [*Izvestiya, Phys. Solid Earth* **33**, 341–357 (1997)].
16. D. M. Pechersky, "Neogeoen Paleomagnetism Constraints on the Processes at the Core and Surface of the Earth," *Russ. J. Earth Sci.* No. 2, (1998); <http://rjes.wdcb.ru>.
17. D. M. Pechersky, "World Magnetic Anomalies and the Amplitude of Secular Variations in the Geomagnetic Field Direction," *Geomagn. Aeron.* **40**, 128–133 (2000).
18. D. M. Pechersky, "The Total Amplitude of Secular Variations, Global Magnetic Anomalies and Plumes," *Fiz. Zemli*, No. 5, 85–91 (2001) [*Izvestiya, Phys. Solid Earth* **37**, 429–435 (2001)].
19. D. M. Pechersky, "Geomagnetic Reversals, Plumes, and Changes in the Organic World in the Phanerozoic: Remarkable Coincidences," *Fiz. Zemli*, No. 1, 53–56 (2003) [*Izvestiya, Phys. Solid Earth* **39**, 48–51 (2003)].
20. D. M. Pechersky, "Geomagnetic Field near Paleozoic–Mesozoic Boundary and Siberian Superplume," *Russ. J. Earth Sci.* **8** (1), (2006); <http://rjes.wdcb.ru>.
21. D. M. Pechersky and A. N. Didenko, *Paleo-Asian Ocean: Petromagnetic and Paleomagnetic Constraints on Its Lithosphere* (OIFZ RAN, Moscow, 1995) [in Russian].
22. D. M. Pechersky and A. V. Garbuzenko, "The Mesozoic–Cenozoic Boundary: Paleomagnetic Characteristic," *Russ. J. Earth Sci.* **7** (2) (2005); <http://rjes.wdcb.ru>.
23. C. R. Scotese and W. S. McKerron, "Revised World Maps and Introduction," in *Paleozoic Paleogeography and Biogeography, Geological Society Memoir No. 12* (1990), pp. 1–21.
24. V. P. Shcherbakov, G. M. Solodovnikov, and N. K. Sycheva, "Variations in the Geomagnetic Dipole during the Past 400 Million Years (Volcanic Rocks)," *Fiz. Zemli*, No. 2, 26–33 (2002) [*Izvestiya, Phys. Solid Earth* **38**, 113–119 (2002)].
25. M. A. Smethurst, A. N. Khramov, and T. H. Torsvik, "The Neoproterozoic and Palaeozoic Palaeomagnetic Data for the Siberian Platform: From Rodinia to Pangea," *Earth-Sci. Rev.* **43**, 1–24 (1998).
26. T. H. Torsvik and R. Van der Voo, "Refining Gondwana and Pangea Palaeogeography: Estimates of Phanerozoic Non-Dipole (Octupole) Fields," *Geophys. J. Int.* **151**, 771–794 (2002).
27. L. P. Zonenshain, M. I. Kuz'min, and M. V. Kononov, "Reconstructions of the Position of Continents in the Paleozoic and Mesozoic," *Geotektonika*, No. 3, 16–27 (1987).